δf Simulation Studies of the Ion-Electron Two-Stream Instability in Heavy Ion Fusion Beams

Hong Qin, Ronald C. Davidson, Edward A. Startsev, and W. Wei-li Lee

Plasma Physics Laboratory, Princeton University, Princeton, NJ 08543, USA

Abstract

Ion-electron two-stream instabilities in high intensity heavy ion fusion beams, described self-consistently by the nonlinear Vlasov-Maxwell equations, are studied using a 3D multispecies perturbative particle simulation method. Large-scale parallel particle simulations are carried out using the recently developed Beam Equilibrium, Stability, and Transport (BEST) code. For a parameter regime characteristic of heavy ion fusion drivers, simulation results show that the most unstable mode of the ion-electron two-stream instability has a dipole-mode structure, and the linear growth rate decreases with increasing axial momentum spread of the beam particles due to Landau damping by an axial momentum spread of the beam ions in the longitudinal direction.

I. INTRODUCTION

In typical linear induction accelerators for heavy ion fusion drivers, the beam current is much higher than that in contemporary accelerators and storage rings. In order to obtain enough fusion energy gain, the peak current for each beam is required to be order of 10^3 A or larger. Even though the kinetic energy is expected to be in the range of several GeV, the reduction of space-charge effects due to the self-magnetic fields is small because of the large ion mass. For a given focusing lattice, most designs of heavy ion fusion drivers operate near the space-charge limit. Large space-charge forces inevitably induce a strong interaction among the beam particles, and in some regimes can result in collective instabilities [1–3]. It has been recognized recently, both in theoretical studies and in experimental observations [2,4-15], that the relative streaming motion of the high-intensity beam particles through a background charge species provides the free energy to drive the classical *two-stream* instability, appropriately modified to include the effects of dc space charge, relativistic kinematics, presence of a conducting wall, etc. A background population of electrons can result by secondary emission when energetic beam ions strike the chamber wall, or through ionization of background neutral gas by the beam ions. A well-documented example is the electron-proton (e-p) instability observed in the Proton Storage Ring experiment [11-12], although a similar instability also exists for other ion species, including (for example) ion-electron interactions in electron storage rings [13-15]. When electrons are present, two-stream interactions in heavy ion fusion drivers are expected to be stronger than the two-stream instabilities observed so far in proton machines (as well as electron machines) because of the much larger beam intensity. In this paper, we study the ion-electron two-stream instability using a perturbative particle simulation method (δf method) for solving the Vlasov-Maxwell equations. As a low-noise nonlinear particle simulation technique [16, 17], the δf method has been implemented in the recently developed Beam Equilibrium, Stability, and Transport (BEST) code [18], which has been applied to a wide range of important collective processes in intense beams [18, 19]. In the present simulation study, we consider a Cs^+ beam with rest mass $m_b = 133\ m_p$, where m_p is the proton rest mass, and kinetic energy $(\gamma_b - 1)mc^2 = 2.5$ GeV, as an example of a heavy ion beam. The paper is organized as follows. In Sec. II, the theoretical model and the physics of the two-stream instability is briefly summarized,

which is followed by a description of the nonlinear δf method in Sec. III. Typical simulation results are presented in Sec. IV, and in Sec. V we summarize the conclusions and describe future work.

II. THEORETICAL MODEL

The theoretical model employed here is based on the nonlinear Vlasov-Maxwell equations. We consider a thin, continuous, high-intensity ion beam ($j = b$), with characteristic radius r_b propagating in the z-direction through background electrons ($j = e$), with each component described by a distribution function $f_j(\mathbf{x}, \mathbf{p}, t)$ [2, 4]. The charge components ($j = b, e$) propagate in the z-direction with characteristic axial momentum $\gamma_j m_j \beta_j c$, where $V_j = \beta_j c$ is the average directed axial velocity, $\gamma_j = (1-\beta_j^2)^{-1/2}$ is the relativistic mass factor, e_j and m_j are the charge and rest mass, respectively, of a j'th species particle, and c is the speed of light in *vacuo*. While the nonlinear δf formalism described in Sec. III is readily adapted to the case of a *periodic* applied focusing field [20], for present purpose we make use of a *smooth-focusing* model in which the applied focusing force is described by $\mathbf{F}_j^{foc} = -\gamma_j m_j \omega_{\beta j}^2 \mathbf{x}_\perp$, where $\mathbf{x}_\perp = x\hat{\mathbf{e}}_x + y\hat{\mathbf{e}}_y$ is the transverse displacement from the beam axis, and $\omega_{\beta j} = const$ is the effective applied betatron frequency for transverse oscillations. Furthermore, in a frame of reference moving with axial velocity $\beta_j c$, the motion of a j'th species particle is assumed to be nonrelativistic. The space-charge intensity is allowed to be arbitrarily large, subject only to transverse confinement of the beam ions by the applied focusing force, and the background electrons are confined in the transverse plane by the space-charge potential $\phi(\mathbf{x}, t)$ produced by the excess ion charge.

In the electrostatic and magnetostatic approximations, we represent the self-electric and self-magnetic fields as $\mathbf{E}^s = -\nabla\phi(\mathbf{x}, t)$ and $\mathbf{B}^s = \nabla \times A_z(\mathbf{x}, t)\hat{\mathbf{e}}_z$. The nonlinear Vlasov-Maxwell equations can be approximated by [2, 4]

$$\left\{ \frac{\partial}{\partial t} + \mathbf{v} \cdot \frac{\partial}{\partial \mathbf{x}} - [\gamma_j \mathrm{m}_j \omega_{\beta j}^2 \mathbf{x}_\perp + e_j(\nabla\phi - \frac{v_z}{c}\nabla_\perp \mathrm{A}_z] \cdot \frac{\partial}{\partial \mathbf{p}} \right\} f_j(\mathbf{x}, \mathbf{p}, t) = 0, \tag{1}$$

and

$$\nabla^2\phi = -4\pi \sum_j e_j \int d^3p f_j(\mathbf{x},\mathbf{p},t),$$
$$\nabla^2 A_z = -\frac{4\pi}{c} \sum_j e_j \int d^3p v_z f_j(\mathbf{x},\mathbf{p},t). \tag{2}$$

Applying the theoretical model outlined above to the ion-electron two-stream instability, Davidson, *et. al.* [1, 2, 4–6] have identified an important class of surface modes driven unstable by ion-electron interactions. A kinetic dispersion relation has been derived for beams with a Kapchinskij-Vladimirskij (KV) distribution in the transverse direction and a Lorentzian distribution in axial momentum in the longitudinal direction [4–6]. A careful examination of the dispersion relation shows that the strongest instability occurs for azimuthal mode number $l = 1$, corresponding to a simple dipole displacement of the beam ions and electrons. The dispersion relation for the $l = 1$ dipole-mode is given by [2, 4–6]

$$[(\omega - k_z V_b + i|k_z|v_{T\|b})^2 - \omega_b^2][(\omega + i|k_z|v_{T\|e})^2 - \omega_e^2] = \omega_f^4 \ , \tag{3}$$

where

$$\omega_f^4 \equiv \frac{1}{4} f \left(1 - \frac{r_b^2}{r_w^2}^2\right) \frac{\gamma_b m_b}{m_e} \hat{\omega}_{pb}^4 \ , \tag{4}$$

$$\omega_e^2 \equiv \frac{1}{2} \frac{\gamma_b m_b}{m_e} \hat{\omega}_{pb}^2 \left(1 - f \frac{r_b^2}{r_w^2}\right) \ , \tag{5}$$

$$\omega_b^2 \equiv \omega_{\beta b}^2 + \frac{1}{2} \hat{\omega}_{pb}^2 \left(f - \frac{1}{\gamma_b^2} \frac{r_b^2}{r_w^2}\right) \ . \tag{6}$$

Here, ω is the complex oscillation frequency, charge state $Z_b = 1$ is assumed, m_e is the electron mass, $\hat{\omega}_{pb}^2 = 4\pi \hat{n}_b e_b^2/\gamma_b m_b$ is the ion plasma frequency-squared on axis, $v_{T\|b}$ and $v_{T\|e}$ are the characteristic longitudinal thermal velocity of the beam ions and electrons, $f \equiv \hat{n}_e/\hat{n}_b$ is the fractional charge neutralization, and k_z is the axial wavenumber. In the cold limit ($v_{T\|b} = 0 = v_{T\|e}$), and in the absence of background electrons ($f = 0$), Eq. (3) gives stable collective oscillations of the ion beam with frequency $\omega - k_z V_b = \pm\omega_b$. For $f \neq 0$, however, the ion and electron modes are coupled by the ω_f^4 term on the right-hand side of Eq. (3), leading to one unstable mode with $\mathrm{Im}\,\omega > 0$ for a certain range of longitudinal wavenumber k_z. The instability is two-stream in nature, and results from the directed ion motion with axial velocity V_b through the background electrons (assumed stationary with $V_e = 0$). Examination of Eq. (3) [2, 4–6] shows that the unstable mode has frequency and

wavenumber closely tuned to $\omega_0 = \omega_e$ and $k_{z0} = (\omega_e + \omega_b)/V_b$. For heavy ion fusion beams ($m_b \gg m_e$), because $\omega_b^2 \ll \omega_e^2$ in the regimes of practical interest, it follows that the phase velocity in the longitudinal direction of the unstable mode is downshifted only slightly from the directed beam velocity V_b, and therefore can be strongly affected by Landau damping effects associated with a longitudinal momentum spread of the beam ions. This fact can be easily demonstrated by analyzing the dispersion relation (3) with finite $v_{T\|b}$ [2, 6]. The $l = 1$ dipole-mode instability predicted by Eq. (3) has features similar to the resistive-hose instability [22] in the collisionless limit. For azimuthal mode number $l = 0$, the two-stream dispersion relations analogous to Eq. (3) have also been derived by Uhm and Davidson [23] for the so-called sausage and hollowing instabilities in the collisionless regime.

III. NONLINEAR δf METHOD

To simulate the ion-electron two-stream instability in a heavy ion beam, it is necessary to use a fully 3D, kinetic, low-noise simulation method. This is because the instability has a 3D mode structure which depends on (x, y, z), and kinetic effects dominate the stabilization process and the nonlinear saturation of the instability. Due to the large mass ratio between the ions and the electrons ($m_e/m_b = 1/(1836 \times 133) = 4.1 \times 10^{-6}$, for cesium), and the fact that the growth rate of the instability is much smaller than the real frequency of the eigenmode, it takes a relatively long time to simulate the instability. The low-noise δf method [16–18] used here is therefore highly desirable. In the δf method, the total distribution function is divided into two parts, $f_j = f_{j0} + \delta f_j$, where f_{j0} is a *known* equilibrium solution ($\partial/\partial t = 0$) to the nonlinear Vlasov-Maxwell equations (1) and (2), and the numerical simulation is carried out to determine the detailed nonlinear evolution of the perturbed distribution function δf_j. This is accomplished by advancing the weight function defined by $w_j \equiv \delta f_j/f_j$, together with the particles' positions and momenta. The equations of motion for the particles, obtained from the characteristics of the nonlinear Vlasov equation (1), are given by

$$\begin{aligned}
\frac{d\mathbf{x}_{\perp ji}}{dt} &= (\gamma_j m_j)^{-1}\mathbf{p}_{\perp ji}, \\
\frac{dz_{ji}}{dt} &= v_{zji} = \beta_j c + \gamma_j^{-3} m_j^{-1}(p_{zji} - \gamma_j m_j \beta_j c), \\
\frac{d\mathbf{p}_{ji}}{dt} &= -\gamma_j m_j \omega_{\beta j}^2 \mathbf{x}_{\perp ji} - e_j \left(\nabla\phi - \frac{v_{zji}}{c}\nabla_\perp A_z\right).
\end{aligned} \tag{7}$$

Here the subscript "ji" labels the i'th simulation particle of the j'th species. The dynamical equations for w_{ji} is given by [16, 18]

$$\begin{aligned} \frac{dw_{ji}}{dt} &= -(1-w_{ji})\frac{1}{f_{j0}}\frac{\partial f_{j0}}{\partial \mathbf{p}}\cdot\delta\left(\frac{d\mathbf{p}_{ji}}{dt}\right), \\ \delta\left(\frac{d\mathbf{p}_{ji}}{dt}\right) &\equiv -e_j\left(\nabla\delta\phi - \frac{v_{zji}}{c}\nabla_\perp\delta A_z\right), \end{aligned} \tag{8}$$

where $\delta\phi = \phi - \phi_0$ and $\delta A_z = A_z - A_{z0}$. Here, the equilibrium solutions (ϕ_0, A_{z0}, f_{j0}) solve the steady-state Vlasov-Maxwell equations (1) and (2). A wide variety of axisymmetric equilibrium solutions to Eqs. (1) and (2) have been investigated in the literature [1, 2]. The perturbed distribution δf_j is obtained through the weighted Klimontovich representation [1],

$$\delta f_j = \frac{N_j}{N_{sj}}\sum_{i=1}^{N_{sj}} w_{ji}\delta(\mathbf{x}-\mathbf{x}_{ji})\delta(\mathbf{p}-\mathbf{p}_{ji}), \tag{9}$$

where N_j is the total number of actual j'th species particles, and N_{sj} is the total number of *simulation* particles for the j'th species. Maxwell's equations are also expressed in terms of the perturbed fields and the perturbed charge and current densities according to

$$\nabla^2\delta\phi = -4\pi\sum_j e_j\delta n_j, \quad \nabla^2\delta A_z = -\frac{4\pi}{c}\sum_j \delta j_{zj}, \tag{10}$$

where

$$\begin{aligned} \delta n_j &= \frac{N_j}{N_{sj}}\sum_{i=1}^{N_{sj}} w_{ji}S(\mathbf{x}-\mathbf{x}_{ji}), \\ \delta j_{zj} &= \frac{e_jN_j}{N_{sj}}\sum_{i=1}^{N_{sj}} v_{zji}w_{ji}S(\mathbf{x}-\mathbf{x}_{ji}). \end{aligned} \tag{11}$$

Here, $S(\mathbf{x}-\mathbf{x}_{ji})$ is a shape function distributing particles on the grids in configuration space. The nonlinear particle simulations are carried out by iteratively advancing the particle motions, including the weights they carry, according to Eqs. (7) and (8), and updating the fields by solving the perturbed Maxwell's equations (10) with appropriate boundary conditions at the cylindrical, perfectly conducting wall ($r = r_w$). Even though it is a perturbative approach, the δf method is *fully nonlinear* and simulates completely the original nonlinear Vlasov-Maxwell equations. Compared with conventional particle-in-cell simulations, the noise level in δf simulations is significantly reduced. The dominant numerical noise mechanisms in particle simulations, such as numerical collisions, are statistical. The

δf method reduces the noise level of the simulations because the statistical noise, which is of order $O(N_s^{-1/2})$ for the total distribution function in the conventional particle-in-cell (PIC) method, is only associated with the perturbed distribution function in the δf method. If the same number of simulation particles is used in the two approaches, then the noise level in the δf method is reduced by a factor of f/δf relative to the PIC method. The δf method can also be used to study *linear* stability properties, provided the factor $(1 - w_{ji})$ in Eq. (8) is approximated by unity, and the forcing terms in Eq. (7) are replaced by the unperturbed force. Implementation of the 3D multispecies nonlinear δf simulation method described above is embodied in the BEST code [18]. For those fast particle motions which require much larger sampling frequency $1/\Delta t$ than the frequency of the mode being studied, the code uses an adiabatic field pusher to advance the particles many time steps without solving for the perturbed fields. The upper limit for Δt, the time step to advance the particles' phase space position, is normally determined by the Courant condition. On the IBM SP-2 supercomputer, the BEST code advances 4.0×10^{11} particles$\times$time-steps in the present study.

IV. SIMULATION RESULTS

In the present simulations of the two-stream instability, instead of using the theoretically-convenient KV distribution [2], we assume that the background equilibrium distribution $(\partial/\partial t = 0)$ is the more realistic *bi-Maxwellian* distribution with temperature $T_{j\perp} = const.$ in the $x - y$ plane, and temperature $T_{j\parallel} = const.$ in the z-direction. That is,

$$
\begin{aligned}
f_{j0}(r, \mathbf{p}) = & \frac{\hat{n}_j}{(2\pi m_j)^{3/2} \gamma_j^{5/2} T_{j\perp} T_{j\parallel}^{1/2}} \\
& \times \exp\left\{ -\frac{(p_z - \gamma_j m_j \beta_j c)^2}{2\gamma_j^3 m_j T_{j\parallel}} \right\} \\
& \times \exp\left\{ -\frac{p_\perp^2/2\gamma_j m_j + \gamma_j m_j \omega_{\beta j}^2 r^2/2 + e_j(\phi_0 - \beta_j A_{z0})}{T_{j\perp}} \right\},
\end{aligned}
\tag{12}
$$

where $\hat{n}_j$ is the density on axis $(r = 0)$ of the j'th species. Here, $V_e = 0$ and $\gamma_e = 1$ for stationary background electrons, and ϕ_0 and A_{z0} are equilibrium self-field potentials,

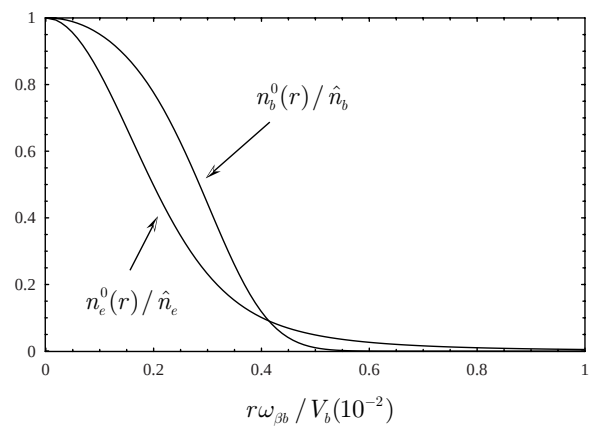

FIG. 1: Plots of the normalized equilibrium beam ion and background electron density profiles.

determined self-consistently from the nonlinear Maxwell equations

$$\frac{1}{r}\frac{\partial}{\partial r}r\frac{\partial\phi_0(r)}{\partial r} = -4\pi\sum_j e_j\int d^3p f_{j0}(r,\mathbf{p}), \tag{13}$$
$$\frac{1}{r}\frac{\partial}{\partial r}r\frac{\partial A_{z0}(r)}{\partial r} = -\frac{4\pi}{c}\sum_j e_j\int d^3p v_z f_{j0}(r,\mathbf{p}).$$

In the simulations, we take $\gamma_b = 1.02$, $m_e/m_b = 1/(1836\times 133) = 4.1\times 10^{-6}$, $V_e = 0$, and $\omega_{\beta e} = 0$ (corresponding to axially stationary electrons). Unlike the KV distribution, which is unstable due to the highly inverted distribution in phase space, a single-species charged particle beam with *bi-Maxwellian* distribution has been proven to be linearly and nonlinearly stable [2, 21] for transverse perturbations with $k_z = 0$. The beam intensity is taken to be near the upper limit, corresponding to $s_b \equiv \hat{\omega}_{pb}^2/2\gamma_b^2\omega_{\beta b}^2 \to 1$. The fractional charge neutralization $f \equiv \hat{n}_e/\hat{n}_b$ is taken to be 10%, where $\hat{n}_e$ and $\hat{n}_b$ are the electron and beam ion densities on axis ($r = 0$). Plotted in Fig. 1 are the normalized equilibrium density profiles for the cesium ions and electrons, $n_j^0(r)/\hat{n}_j = (1/\hat{n}_j)\int d^3p f_{j0}(r,\mathbf{p},t)$ $(j = b, e)$, which are readily obtained once the equilibrium potentials ϕ_0 and A_{z0} are solved numerically from Eqs. (12) and (13). The transverse temperatures of the electrons and ions in Fig. 1 are chosen to be $T_{b\perp}/\gamma_b m_b V_b^2 = 1.1\times 10^{-6}$ and $T_{e\perp}/\gamma_b m_b V_b^2 = 2.6\times 10^{-6}$, such that the ion and electron density profiles overlap radially. The overlapping of the electron density profile with that of the ions is expected to maximize the two-stream interaction and therefore the growth rate. In the space-charge limit ($s_b = 1$), if there is no electron population, the beam would have a flat-top density profile. However, the presence of electrons offsets some of the space-charge force and produces the bell-shape beam density profile in Fig. 1.In the simulations, after

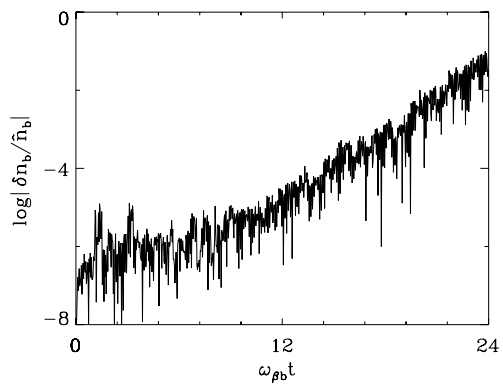

FIG. 2: Time history of pertubed desnity $\delta n_b/\hat{n}_b$ at a fixed spatial location. After an initial transition period, the $l = 1$ dipole-mode perturbation grows exponentially.

small-amplitude perturbations are excited at $t = 0$, the system is evolved self-consistently for thousands of wave periods. Plotted in Fig. 2 is the time history of the beam density perturbation at one spatial location in a simulation using the *linearized* version of the BEST code. Evidently, after an initial transition period, the perturbation grows exponentially, which is the expected behavior of an instability during the linear growth phase. In Fig. 3, the $x-y$ projection of the perturbed potential $\delta\phi$ at a fixed longitudinal position are plotted at $t = 0$ and $t = 12.8/\omega_{\beta b}$. Clearly, $\delta\phi$ grows to a moderate amplitude by $t = 12.8/\omega_{\beta b}$, and the $l = 1$ dipole mode is the dominant unstable mode, for which the growth rate is measured to be $\mathrm{Im}\,\omega = 0.58\omega_{\beta b}$. The real eigenfrequency of the mode is $\mathrm{Re}\,\omega = 361\omega_{\beta b}$, and the normalized wavelength at maximum growth is $k_z V_b/\omega_{\beta b} = 361.3$.

In the simulation results for the two-stream instability presented above, we have assumed initially cold beam ions in the longitudinal direction ($\Delta p_{b\|}/p_{b\|} = 0$) to maximize the growth rate of the instability. Here, $p_{b\|} = \gamma_b m_b V_b$. In general, when the longitudinal momentum spread of the beam ions is finite, Landau damping by parallel ion kinetic effects provides a mechanism that reduces the growth rate. Shown in Fig. 4 is a plot of the maximum linear growth rate $(Im\omega)_{max}$ versus the normalized initial axial momentum spread $\Delta p_{b\|}/p_{b\|}$ obtained in the numerical simulations. As evident from Fig. 4 , the growth rate decreases dramatically as $\Delta p_{b\|}/p_{b\|}$ is increased. When $\Delta p_{b\|}/p_{b\|}$ is high enough, about 0.235% for the case in Fig. 4, the mode is completely stabilized by longitudinal Landau damping effects by the beam ions. This result agrees with theoretical predications. Because the phase velocity of the unstable mode in the longitudinal direction is far removed from the electron velocity

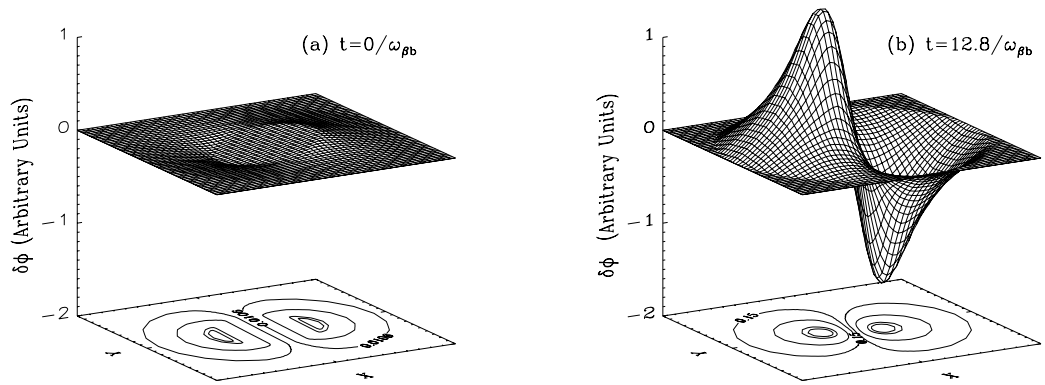

FIG. 3: The x-y projection (at fixed value of z) of the perturbed electrostatic potential $\delta\phi(x, y, t)$ for the ion-electron two-stream instability growing from a small initial perturbation, shown at (a) $t = 0$, and (b) $\omega_{\beta b}t = 12.8$.

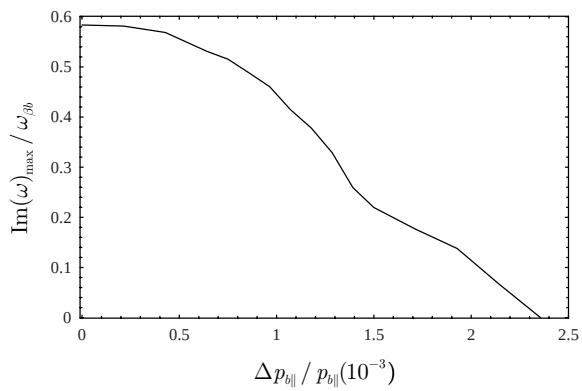

FIG. 4: The maximum linear growth rate $(\mathrm{Im}\,\omega)_{max}$ of the ion-electron two-stream instability decreases as the longitudinal momentum spread of the beam ions increases.

distribution $\mid \omega/k_z \mid \gg V_e + v_{Te\|}$, we do not expect the longitudinal electron temperature to significantly affect the growth rate of the instability.

V. CONCLUSIONS AND FUTURE RESEARCH

In this paper, we have studied the linear growth phase of the ion-electron two-stream instability in a high intensity heavy ion fusion beam using a perturbative particle simulation method (δf method) for solving the Vlasov-Maxwell equations. As a low-noise nonlinear particle simulation technique, the δf method is an ideal tool for simulating the two-stream instability which requires the capability of self-consistently evolving small perturbed field quantities for millions of time steps. Large-scale parallel particle simulations have been

carried out using the recently developed BEST code.The simulation results show that the most unstable mode of the two-stream instability has a dipole structure, and that the linear growth rate decreases with increasing axial momentum spread of the beam particles due to Landau damping by the beam ions in the longitudinal direction. Further studies are necessary to better understand the linear and nonlinear properties of the two-stream instability for heavy ion fusion parameters. In the linear regime, the dependence of the instability threshold on momentum spread and fractional charge neutralization, and the additional damping mechanism due to transverse tune spread are important questions that need to be investigated. Nonlinearly, it is essential to understand the nonlinear saturation level, and the possible subsequent nonlinear evolution of the system. Results in these areas will be reported in future publications.

Acknowledgments

This research was supported by the U.S. Department of Energy.

---

[1] Davidson, R. C. (2001), *Physics of Nonneutral Plasmas* (World Scientific, 2001), and references therein.

[2] Davidson, R. C., and Qin, H. (2001), *Physics of Intense Charged Particle Beams in High Energy Accelerators* (World Scientific, 2001).

[3] Chao, A. W. (1993), *Physics of Collective Beam Instabilities in High Energy Accelerators* (Wiley, New York, 1993).

[4] Davidson, R. C., and Qin, H., Stoltz, P. H., and Wang, T.-S. (1999), Phys. Rev. Special Topics on Accel. and Beams **2**, 054401, and references therein.

[5] Davidson, R. C., Qin, H., and Wang, T.-S. (1999), Phys. Lett. A **252**, 213.

[6] Davidson, R. C., and Qin, H. (2000), Phys. Lett. **A 270**, 177.

[7] Wang, T.-S, Channell, P. J., Macek, R. J., and Davidson, R. C. (2001), Proc. 2001 Particle Accelerator Conference, p.704.

[8] Koshkarev, D. G., and Zenkevich, P. R. (1972), Particle Accel. **3**, 1.

[9] Keil, E., and Zotter, B. (1971), CERN Report CERN-ISR-TH/71-58.

[10] Laslett, L. J., Sessler, A. M., and Möhl, D. (1974), Nucl. Instr. Meth. Phys. Res. **A 121**, 517.

[11] Neuffer, D., Colton, E., Fitzgerald, D., Hardek, T., Hutson, R., Macek, R., Plum, M., Thiessen, H., and Wang, T. -S. (1992), Nucl. Instr. Meth. Phys. Res. **A321**, 1.

[12] Macek, R. J., *et al (2001)*, Proc. 2001 Particle Accelerator Conference, p.668.

[13] Izawa, M., Sato, Y., and Toyomasu, T. (1995), Phys. Rev. Lett. **74**, 5044.

[14] Byrd, J., Chao, A., Heifets, S., Minty, M., Roubenheimer, T. O., Seeman, J., Stupakov, G., Thomson, J., and Zimmerman, F. (1997), Phys. Rev. Lett. **79**, 79.

[15] Ohmi, K. (1997), Phys. Rev. E **55**, 7550.

[16] Lee, W. W., Qian, Q., and Davidson, R. C. (1997), Phys. Lett. **A 230**, 347; Qian, Q., Lee, W. W., and Davidson, R. C. (1997), Phys. Plasmas **4**, 1915.

[17] Stoltz, P. H., Davidson, R. C., and Lee, W. W. (1999), Phys. Plasmas **6**, 298.

[18] Qin, H., Davidson, R. C., and Lee, W. W. (2000), Phys. Rev. Special Topics on Accel. and Beams **3**, 084401; **3**, 109901.

[19] Startsev, E., Davidson, R. C., and Qin, H. (2002), Phys. Plasmas **9**, in press.

[20] Davidson, R. C., Qin, H., and Channell, P. J. (1999), Phys. Rev. Special Topics on Accel. and Beams **2**, 074401; **3**, 029901; Channell, P. J. (1999), Phys. Plasmas **6**, 982.

[21] Davidson, R. C. (1998), Phys. Rev. Lett. **81**, 99; Davidson, R. C. (1998), Phys. Plasmas **5**, 3459.

[22] Lee, E. P. (1978), Phys. Fluids **2**1, 1327.

[23] Uhm, H. S., Davidson, R. C., and Kaganovich, I. (2001), Phys. Plasmas **8**, 4637.